

# Performances of Hybrid Amplitude Shape Modulation for UWB Communications Systems over AWGN Channel in a Single and Multi-User Environment

Marijan HERCEG, Tomislav MATIĆ, Tomislav ŠVEDEK

Dept. of Communication, Faculty of Electrical Engineering, J. J. Strossmayer University of Osijek, Kneza Trpimira 2b, Osijek, Croatia

marijan.herceg@etfos.hr, tomislav.matic@etfos.hr, tomislav.svedek@etfos.hr

**Abstract.** This paper analyzes the performance of the hybrid Amplitude Shape Modulation (h-ASM) scheme for the time-hopping ultra-wideband (TH-UWB) communication systems in the single and multi-user environment. h-ASM is the combination of Pulse Amplitude Modulation (PAM) and Pulse Shape Modulation (PSM) based on modified Hermite pulses (MHP). This scheme is suitable for high rate data transmission applications because  $b = \log_2(MN)$  bits can be mapped with one waveform. The channel capacity and error probability over AWGN channel are derived and compared with other modulation schemes.

## Keywords

Ultra-Wideband, Pulse-Amplitude Modulation, Pulse-Shape Modulation.

## 1. Introduction

UWB [1] radio systems have recently gained increased popularity due to their low power consumption, high speed transmission and anti-interference characteristics. In UWB systems, symbols are transmitted with very short pulses ( $< 2$  ns), which spread energy of the signal up to 10 GHz. The pulses must be formed to satisfy power and spectrum regulations defined by the Federal Communications Commission (FCC) [2]. To obtain desired power and spectral ranges different types of pulse shapes are used [3], [4]. The most commonly used pulses are derivation of Gaussian monocycle and modified Hermite pulses (MHP) often called Hermites [5]. Different modulation techniques such as PAM, Pulse Position Modulation (PPM), PSM, On-Off-Keying (OOK), Biphase Modulation (BPM) are used in TH-UWB systems. To achieve better system performance such as higher data rate, less complex receiver and less power consumption, combined modulation techniques such as Pulse Position Amplitude Modulation (PPAM) [6], Biorthogonal Pulse Position Modulation (BPPM) [7], OOK-PSM [8], PPM-PSM [9] and hybrid

Shape, Amplitude and Position Modulation [10] are proposed. In PAM and OOK modulation information is contained in the amplitude of a signal, PPM uses position of an impulse to convey information, and in PSM modulation, information is conveyed in the shape of pulse.

PSM modulation is interesting due to its robustness to the inter symbol interference (ISI), but on the other hand the autocorrelation properties for higher order orthogonal pulses [11] makes the PSM unsuitable for higher order modulation scheme. Furthermore it requires  $M$  correlators in the receiver for an  $M$ -ary PSM. To solve these problems and to increase the bit-rate the hybrid  $MN$ -ary h-ASM modulation scheme based on orthogonal pulses is proposed.  $MN$ -ary h-ASM waveform consists of  $N$  orthogonal signals with  $M$  amplitude levels for each signal. This paper is organized as follows: Section 2 describes basic properties of the  $MN$ -ary h-ASM modulation scheme. In section 3, MHP are described, section 4 shows the performance and channel capacity for single user over AWGN channel, section 5 presents performance in multi user environment. In section 6, the UWB link budget model is presented, while section 7 shows performance simulation results of the  $MN$ -ary h-ASM modulation. Some conclusions are given in section 8.

## 2. $MN$ -ary h-ASM Modulation Basics

The  $MN$ -ary h-ASM transmitter and receiver scheme is shown in Fig. 1. and Fig. 2. Transmitter maps  $b = \log_2(MN)$  bits in one  $MN$ -ary h-ASM waveform. Each waveform consists of an  $n$ -th orthogonal MHP pulse with an  $m$ -th discrete amplitude level. The overall transmitted signal of the  $k$ -th user in time-hopping format can be defined as:

$$s^{(k)}(t) = \sqrt{E_t} \sum_{j=-\infty}^{\infty} A_{\lfloor \frac{j}{N_s} \rfloor}^{(k)} w_{d_{\lfloor \frac{j}{N_s} \rfloor}}^{(k)}(t - jT_f - c_j^{(k)}T_c) \quad (1)$$

where  $b_{\lfloor \frac{j}{N_s} \rfloor} \in \{1, 2, \dots, M\}$ ,  $d_{\lfloor \frac{j}{N_s} \rfloor} \in \{0, 1, \dots, (N-1)\}$ ,  $\lfloor \cdot \rfloor$  is the integer floor operator,  $A_{b_{\lfloor \frac{j}{N_s} \rfloor}} \sqrt{E_t}$  is one of the possible amplitude levels where  $A_{b_{\lfloor \frac{j}{N_s} \rfloor}} = 2^{b_{\lfloor \frac{j}{N_s} \rfloor} - 1 - M}$ ,  $E_t = 3E_{av}/(M^2 - 1)$ ,

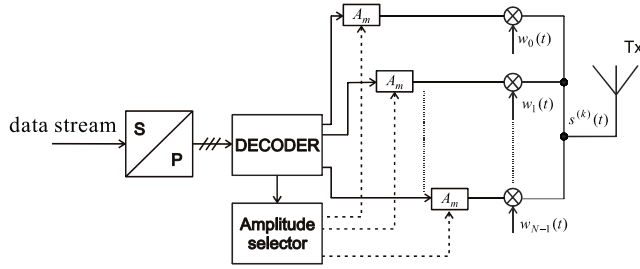


Fig. 1. h-ASM transmitter.

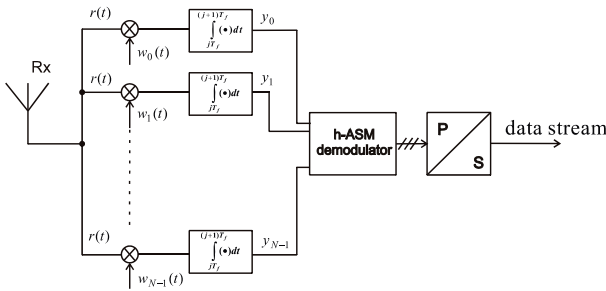


Fig. 2. h-ASM receiver.

and  $E_{av}$  is the average signal energy.  $T_f$  is a frame time, which is hundred to thousand times the pulse duration.  $N_s$  is the number of pulses used to transmit one symbol, where the symbol period is  $T_s = N_s T_f$ .  $c_j^{(k)}$  is the TH sequence with chip duration  $T_c$ , which provides additional shift in order to avoid catastrophic collisions due to multi user interference (MUI) and

$$w_d \left[ \frac{j}{N_s} \right] (t) \in \{w_0(t), w_1(t), \dots, w_{N-1}(t)\}, \quad (2)$$

is one of the unit energy orthogonal pulses. Receiver structure is formed from  $N$  correlators followed by a demodulator, where each correlator uses different MHP as template.

### 3. Orthogonal Modified Hermite Pulses

Charles Hermite was born in 1822 in France and some of his mathematical ideas are still widely used today, especially the Hermitian Forms that are used in physics and mathematics. In our particular interest are Hermitian polynomials that are defined with [5]

$$h_{en}(t) = (-\eta T_p)^n e^{t^2/2(\eta T_p)^2} \frac{d^n}{dt^n} (e^{-t^2/2(\eta T_p)^2}) \quad (3)$$

where  $\eta = \sqrt{0.01}$  is the normalization parameter such that 99% of the pulse energy is contained in the range of  $T_p$ , where  $T_p$  is the pulse duration,  $n = 0, 1, 2, \dots$  and  $-\infty < t < \infty$ . Hermite polynomials are not orthogonal, but they can be modified to become orthogonal ones as follows

$$h_n(t) = k_n e^{-t^2/4(\eta T_p)^2} h_{en}(t) \quad (4)$$

where  $k_n$  is the constant which determines the pulse energy and it is defined by

$$k_n = \sqrt{\frac{E_n}{\eta T_p n! \sqrt{2\pi}}} \quad (5)$$

where  $E_n$  is the energy of the  $n$ -th pulse. The functions defined in (4) are called modified Hermite pulses (MHP). Fig. 3. shows the first and third MHP with pulse duration  $T_p = 1$  ns normalized to unit energy.

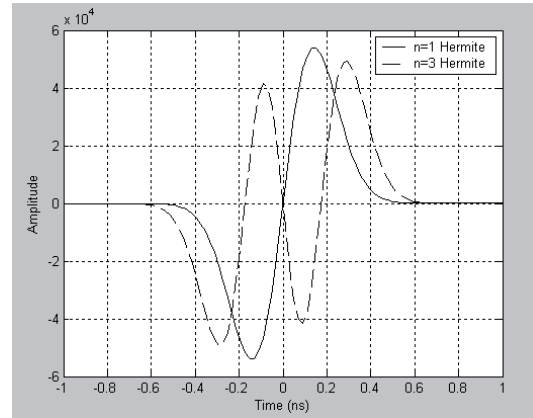


Fig. 3. The first and third modified Hermite pulses (MHP).

These two pulses are interesting due to their properties: the pulse duration is almost the same, the pulse bandwidth is almost the same, the pulses are mutually orthogonal, and have zero DC components.

The autocorrelation and cross-correlation functions, obtained by Mathematica 5.1, are shown in Fig. 4. and given by

$$R_{1,1}(\Delta t) = \left( 1 - \frac{\Delta t^2}{4(\eta T_p)^2} \right) e^{-\Delta t^2 / (8(\eta T_p)^2)}, \quad (6)$$

$$R_{3,3}(\Delta t) = \left( 1 - \frac{3\Delta t^2}{4(\eta T_p)^2} + \frac{3\Delta t^4}{32(\eta T_p)^4} - \frac{\Delta t^6}{384(\eta T_p)^6} \right) e^{-\Delta t^2 / (8(\eta T_p)^2)}, \quad (7)$$

$$R_{1,3}(\Delta t) = \frac{\sqrt{6}}{12(\eta T_p)^2} \Delta t^2 \left( 1 - \frac{\Delta t^2}{12(\eta T_p)^2} \right) e^{-\Delta t^2 / (8(\eta T_p)^2)}. \quad (8)$$

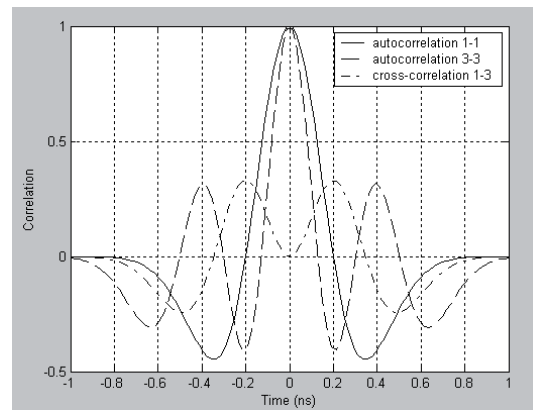


Fig. 4. Autocorrelation and cross-correlation functions of the first and third MHP.

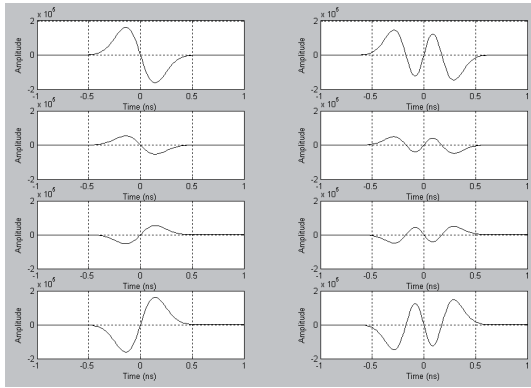


Fig. 5. All possible waveforms for 4x2 h-ASM.

Fig. 5. shows an example of all possible waveforms for four amplitude levels  $\{\pm 3, \pm 1\}$  and two shapes  $\{\text{MHP1}, \text{MHP3}\}$  h-ASM (4x2 h-ASM).

#### 4. Performance of $MN$ -ary h-ASM in Single User Environment

The received signal in additive white Gaussian noise (AWGN) channel in single-user environment can be written as

$$r(t) = s^{(1)}(t - \tau^{(1)}) + n(t) \quad (9)$$

where  $\tau^{(1)}$  is the time delay of the first user,  $n(t)$  is the AWGN noise with zero mean value and variance  $N_0/2$ . On the input of each correlator the received signal is multiplied by a template signal and decision is made on the basis on the cross and autocorrelation properties of the orthogonal pulses.

When the  $n$ -th pulse with the  $m$ -th amplitude level is sent the received signal at the  $i$ -th correlator is given by

$$r_i = \sum_{j=pN_s+1}^{(p+1)N_s} \int_{(j-1)T_f}^{jT_f} r(t) w_i^{(1)}(t - jT_f - c_j^{(1)}) dt, \quad (10)$$

$$i=0, 1, 2, \dots, (N-1).$$

From (10) the signal at the input of a demodulator is

$$r_i = \begin{cases} A_m N_s \sqrt{E_t} + n_n, & i = n \\ n_i, & i \neq n, \end{cases} \quad (11)$$

where  $n_i$  is the AWGN component at the  $i$ -th correlator with zero mean and variance

$$\sigma_n^2 = E[(n_i)^2]$$

$$= \sum_{j=iN_s+1}^{(i+1)N_s} E \left[ \left( n(t) \int_{(j-1)T_f}^{jT_f} w_i^{(1)}(t - jT_f - c_j^{(1)} T_c - \tau^{(1)}) \right)^2 \right] \quad (12)$$

$$= \frac{N_s N_0}{2}.$$

$$C = \log_2 MN - \frac{1}{MN} \sum_{m=1}^M \sum_{n=1}^N E_{r|s_{mn}} \left[ \log_2 \left( \sum_{p=1}^M \sum_{q=1}^N \exp \left( -\frac{r_n^2 - r_q^2 + (r_q - A_p N_s \sqrt{E_t})^2 - (r_n - A_m N_s \sqrt{E_t})^2}{2\sigma^2} \right) \right) \right] \quad (16)$$

For orthogonal signals with equal energy, optimum detector selects the signal resulting with the largest cross-correlation between the received signal  $r(t)$  and each of the possible  $N$  transmitted signals [12]. After the signal with the largest cross-correlation is selected the detector decides which amplitude level is sent according to threshold  $\alpha_m$  levels given for  $M$ -ary PAM as:

$$\alpha_m = \begin{cases} [-\infty, (A_m + 1)N_s \sqrt{E_t}], & m = 1 \\ [(A_m - 1)N_s \sqrt{E_t}, (A_m + 1)N_s \sqrt{E_t}], & m = 2, \dots, M-1 \\ [(A_m - 1)N_s \sqrt{E_t}, \infty], & m = M. \end{cases} \quad (13)$$

The received signal  $r_i$  is an  $N$  dimensional vector with joint Gaussian distribution conditioned by  $s_{mn}$ , where  $s_{mn}$  represents the  $n$ -th pulse with the  $m$ -th amplitude level. The probability density function (PDF) is given by [12], [13]

$$p(r | s_{mn}) = \left( \frac{1}{2\pi\sigma^2} \right)^{N/2} \times \exp \left( -\frac{(r_n - A_m \sqrt{E_t})^2}{2\sigma^2} \right) \prod_{i=1, i \neq n}^N \exp \left( -\frac{r_i^2}{2\sigma^2} \right). \quad (14)$$

In the single-user environment where the AWGN is the only source of distortion  $\sigma^2 = \sigma_n^2$ , the channel capacity for discrete valued inputs and continuous valued output is given by [6], [11], [12]

$$C = \log_2 MN - \frac{1}{MN} \sum_{m=1}^M \sum_{n=1}^N \int_r P(r | s_{mn}) \times \log_2 \left( \frac{\sum_{p=1}^M \sum_{q=1}^N P(r | s_{pq})}{P(r | s_{mn})} \right) dr. \quad (15)$$

The capacity over AWGN channel is obtained from (14), (15) and given as (16) at the bottom of the page.

Due to the (13) and (14) the probability for the correct decision of  $MN$ -ary h-ASM can be written from [12] as:

$$P_c = \frac{1}{M} \left( \int_{-\infty}^{(A_1+1)N_s \sqrt{E_t}} \left( \frac{1}{\sqrt{2\pi}} \int_{\frac{|r_1|}{\sigma}}^{\frac{|r_1|}{\sigma}} e^{-x^2/2} dx \right)^{N-1} p(r_1) dr_1 + \right.$$

$$\left. \int_{(A_m-1)N_s \sqrt{E_t}}^{(A_m+1)N_s \sqrt{E_t}} \left( \frac{1}{\sqrt{2\pi}} \int_{\frac{|r_m|}{\sigma}}^{\frac{|r_m|}{\sigma}} e^{-x^2/2} dx \right)^{N-1} p(r_m) dr_m + \right.$$

$$\left. \int_{(A_M-1)N_s \sqrt{E_t}}^{\infty} \left( \frac{1}{\sqrt{2\pi}} \int_{\frac{|r_M|}{\sigma}}^{\frac{|r_M|}{\sigma}} e^{-x^2/2} dx \right)^{N-1} p(r_M) dr_M \right), \quad (17)$$

where is

$$p(r_m) = \frac{1}{\sqrt{2\pi\sigma^2}} e^{-\frac{(r_m - A_m N_s \sqrt{E_t})^2}{2\sigma^2}} \quad (18)$$

The error probability is then given by

$$P_{MN} = 1 - P_C \quad (19)$$

## 5. Performance of MN-ary h-ASM in Multi-User Environment

In multi-user environment the received signal can be represented with

$$r(t) = \sum_{k=1}^{N_u} s^{(k)}(t - \tau^{(k)}) + n(t) \quad (20)$$

where  $N_u$  is the number of users,  $\tau^{(k)}$  is the time delay of the  $k$ -th user. We may assume that the desired user is the user with  $k = 1$ , that the time delay  $\tau_k$  is uniformly distributed over  $[0, T_f]$  and that  $\tau_k$  is known at the receiver. If the  $n$ -th pulse shape with the  $m$ -th amplitude level is sent, the output of each cross correlator will be

$$r_i = \begin{cases} A_m^{(1)} N_s \sqrt{E_t} + n_{MUI\_n} + n_n, & i = n \\ n_{MUI\_i} + n_i, & i \neq n, \end{cases} \quad (21)$$

where  $n_{MUI\_n}$  is the multi-user interference noise given for the  $p$ -th symbol. The output of the  $n$ -th correlator will be

$$\begin{aligned} n_{MUI\_n} &= \sqrt{E_t} \sum_{k=2}^{N_u} \sum_{j=pN_s+1}^{(p+1)N_s} A_b^{(k)} \left[ \frac{j}{N_s} \right] \\ &\times \int_{(j-1)T_f}^{jT_f} w_i^{(k)}(t - jT_f - c_j^{(k)}T_c - \tau^{(k)}) \\ &\times w_n^{(1)}(t - jT_f - c_j^{(1)}T_c - \tau^{(1)}) \\ &= \sqrt{E_t} \sum_{k=2}^{N_u} \sum_{j=pN_s+1}^{(p+1)N_s} A_b^{(k)} \left[ \frac{j}{N_s} \right] R_{l,n}(\delta_j^{(k)}), \end{aligned} \quad (22)$$

where  $R_{l,n}(\delta_j^{(k)})$  is a cross-correlation function between the  $l$ -th and  $n$ -th pulse,  $\delta_j^{(k)} = (c_j^{(1)} - c_j^{(k)})T_c - (\tau_1 - \tau_k)$  is uniformly distributed random variable over  $[-T_f, T_f]$ , and it represents the difference in pulse time arrival between user 1 and user  $k$ . Note that when  $l = n$  the term  $R_{l,n}(\delta_j^{(k)})$  becomes autocorrelation function  $R_{n,n}(\delta_j^{(k)})$ . Because all pulse shapes are equally likely to occur, the average amount of MUI on each correlator is the average value between autocorrelation and cross correlation. From [14],  $n_{MUI}$  is the zero mean random variable with Gaussian distribution. The variance of  $n_{MUI\_i}$  for the first and third MHP is obtained using Mathematica 5.1 from (6), (7), (8) and are given by

$$\begin{aligned} \sigma_{MUI\_Hermite1}^2 &= \sum_{k=2}^{N_u} \sum_{j=pN_s+1}^{(p+1)N_s} E \left[ \left( A_b^{(k)} \left[ \frac{j}{N_s} \right] \sqrt{E_t} R_{1,1}(\delta_j^{(k)}) \right)^2 \right] \\ &= \frac{3T_p}{4T_f} \sqrt{0.01\pi} (N_u - 1) N_s E_{av} \quad , \end{aligned} \quad (23)$$

$$\begin{aligned} \sigma_{MUI\_Hermite3}^2 &= \sum_{k=2}^{N_u} \sum_{j=pN_s+1}^{(p+1)N_s} E \left[ \left( A_b^{(k)} \left[ \frac{j}{N_s} \right] \sqrt{E_t} R_{3,3}(\delta_j^{(k)}) \right)^2 \right] \\ &= \frac{147T_p}{256T_f} \sqrt{0.01\pi} (N_u - 1) N_s E_{av} \quad , \end{aligned} \quad (24)$$

$$\begin{aligned} \sigma_{MUI\_Hermite1-3}^2 &= \sum_{k=2}^{N_u} \sum_{j=pN_s+1}^{(p+1)N_s} E \left[ \left( A_b^{(k)} \left[ \frac{j}{N_s} \right] \sqrt{E_t} R_{1,3}(\delta_j^{(k)}) \right)^2 \right] \\ &= \frac{1056T_p}{6912T_f} \sqrt{0.01\pi} (N_u - 1) N_s E_{av}. \end{aligned} \quad (25)$$

From (23), (24) and (25) it can be seen that the amount of MUI interference increases with  $N_u$ , and decreases with the pulse spreading gain  $N_c = T_f/T_p$ .  $n_i$  is AWGN noise at the  $i$ -th correlator with zero mean and variance  $\sigma_n^2 = N_s N_0 / 2$ .

According to the equations (23), (24) and (25) we may say that the signal at the input to the demodulator is Gaussian distributed random variable defined as

$$r_i = \begin{cases} N(A_m^{(1)} N_s \sqrt{E_t}, \sigma_{MUI\_Hermite\_n}^2 + \sigma_n^2) & i = n \\ N(0, \sigma_{MUI\_Hermite\_i}^2 + \sigma_n^2) & i \neq n. \end{cases} \quad (26)$$

The error probability and channel capacity in multi user environment can be obtained from (16), (17), (18), (19) by substituting

$$\sigma^2 = \sigma_{MUI\_Hermite\_i}^2 + \sigma_n^2 \quad (27)$$

## 6. UWB Link under FCC Part 15 Rules

In May 2000, the FCC included UWB emissions under Part 15 rule. That rule restricts emissions above 900 MHz to field strength level of  $E = 500 \mu\text{V/m/MHz}$  measured at a distance of 3 m from the transmitter. That restriction constrains the transmitted power of UWB system over a 1 GHz bandwidth to [15]

$$P_t \leq -11 \text{ dBm}. \quad (28)$$

Due to the power constrain the common link budget model from [15] is given from as

$$\frac{SNR}{PG} \leq Pt - N - F - PL \quad , \quad (29)$$

where  $SNR$  is the signal-to-noise ratio,  $PG = N_s T_f W_p$  is the processing gain, and  $W_p$  is the bandwidth of the UWB pulse.  $N = kTW_p$  is the received noise power,  $k$  is Boltzmann's constant,  $T$  is the room temperature (typically taken as 300 K),  $F$  is the noise figure assumed to be  $F = 5 \text{ dB}$ .  $PL$  is the path loss [12] given by

$$PL = 10 \log \left( \frac{4\pi d}{\lambda} \right)^2 \quad (\text{dB}), \quad (30)$$

where  $z$  is the power attenuation exponent,  $\lambda$  is the wavelength corresponding to the working frequency  $f_c$ , which is the center frequency of the pulse.

### 7. Simulation Results

Due to the very complex mathematical expression of error probability (17), (18), (19) and channel capacity (16), the results are obtained using Monte Carlo simulation which is detailed explained in [16]. For all simulation we assumed that all pulses are orthogonal with unit energy, and that there is a perfect synchronization and power control between the transmitter and receiver.

In Fig. 6, the bit-error-rate (BER) of  $MN$ -ary h-ASM is compared with different PPM-PSM [9], H-4, H-8 [10], PPM and PAM modulation schemes. This shows that 2x2 h-ASM has significantly better performance than 2-bit PPM-PSM, 4-PAM, 4-PPM and 0.2 dB worse than H-4 scheme. 2x4 h-ASM is better than 3-bit PPM-PSM, 8-PAM, 8-PPM and 0.5 dB worse than H-8. On the other hand, it is shown that with the increase of the number of the amplitude levels  $M$ , performance has slightly decreased which can be seen if we compare the performance of 4x2 h-ASM with the 2x4 h-ASM.

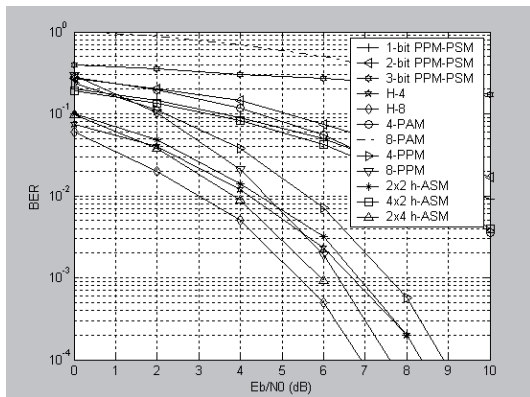


Fig. 6. Performance of  $MN$ -ary h-ASM over AWGN channel.

Fig. 7 shows the channel capacity vs. SNR for the different  $MN$ -ary h-ASM modulation schemes. Compared with other modulation schemes [17] it is shown that the 1x2 h-ASM has approximately the same performance as 2-PPM and 3 dB worse than 2-PSK and 2-PAM. The 2x2 h-ASM has approximately the same performance as 4-PSK and 4-PPM, but 3 dB better than 4-PAM. Moreover, 2x4 h-ASM is approximately the same as 8-PSK and 8-PPM, but 6 dB better than 8-PAM. It is shown that  $MN$ -ary h-ASM with less amplitude levels  $M$  achieve full capacity at the lower SNR which can be seen on the examples given for the 2x4 and 4x2 h-ASM modulation where full capacity is achieved for SNR ratio 10 dB and 15 dB, respectively.

Fig. 8 illustrates the dependency of channel capacity over the distance. The common link budget is given with (28), (29), (30). It is shown that  $MN$ -ary h-ASM modulation with  $M = 2$  can retain full capacity at a distance of 75 m, while at  $MN$ -ary h-ASM modulation with  $M = 4$  the

distance at which the channel capacity is full is double decreased.

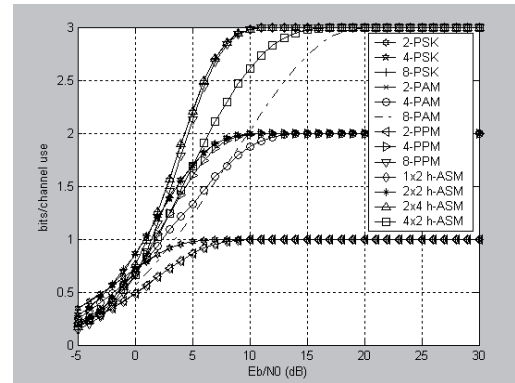


Fig. 7. Channel capacity of  $MN$ -ary h-ASM compared with other modulation schemes.

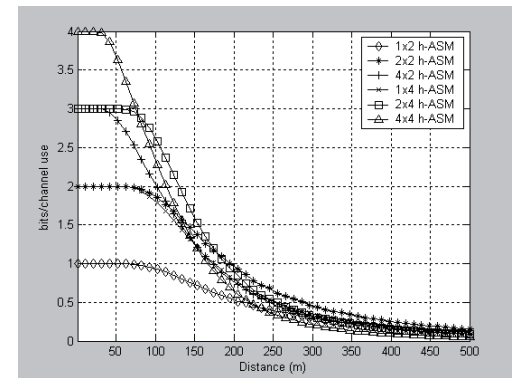


Fig. 8. Channel capacity as the function of the distance with  $z = 2$  and  $PG = 100$ .

Fig. 9 shows an influence of the number of users on the channel capacity for different pulse spreading gains  $N_c$ . It is shown that  $MN$ -ary h-ASM with more amplitude levels  $M$  is not suitable for multi user environment. On the other hand the trade-off between bit-rate and  $N_c$  can adjust  $MN$ -ary h-ASM for a large number of users.

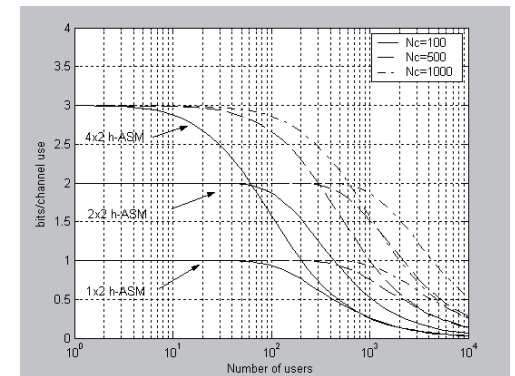


Fig. 9. Channel capacity for different number of users and pulse spreading gain  $N_c$  with  $N_s = 1$ ,  $SNR = 20$  dB,  $T_p = 1$  ns.

Fig. 10 represents the performance of  $MN$ -ary h-ASM from the perspective of error probability in the multi user environment. It is clearly shown how BER increases as the number of users increases.

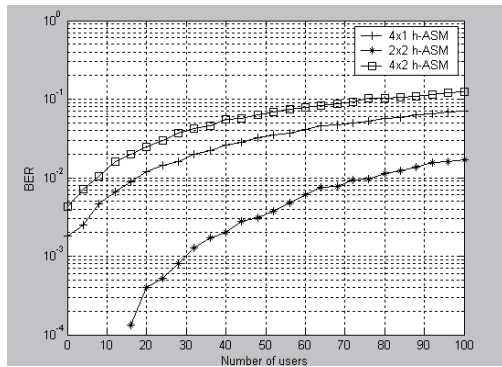


Fig. 10. Performance of  $MN$ -ary h-ASM in multi user environment over AWGN channel,  $N_s = 1$ ,  $\text{SNR}/b = 10$  dB,  $N_c = 100$ .

## 8. Conclusion

This paper shows the performance of hybrid  $MN$ -ary h-ASM modulation scheme over the AWGN channel in the single and multi user environment. It is shown that  $MN$ -ary h-ASM provides better performance than PPM-PSM,  $M$ -ary PAM and  $N$ -ary PPM and slightly worse than H-4, H-8 regard to the BER. When the number of orthogonal pulses  $N$  increases, the performance of  $MN$ -ary h-ASM increases as well, whereas the increase of the number of amplitude levels  $M$ , results in the  $MN$ -ary h-ASM performance decreases. It is also shown that trade-off between  $M$  and  $N$  can customize  $MN$ -ary h-ASM modulation scheme for different applications, from ultra high data-rate applications on short distance, to long distance medium and low data-rate applications. It is also shown that due to the cross and autocorrelation properties of orthogonal pulses,  $MN$ -ary h-ASM with different  $N_c$  is suitable for usage in both, single and multi user environment. We have also shown that hardware complexity can be reduced if the number of amplitude levels increases, when the number of orthogonal pulses decreases (less correlators at the receiver), at the cost of the BER. The advantage of  $MN$ -ary h-ASM over modulation that uses PPM [6], [7], [9], [10] is that the information is not conveyed in position of the pulse, but just in shape, which allows the  $MN$ -ary h-ASM to achieve even higher bit-rates. This property makes the  $MN$ -ary h-ASM modulation scheme very attractive for TH-UWB communication systems.

## Acknowledgements

The research described in the paper was financially supported by the Ministry of Science, Education and Sports of the Republic of Croatia under project 165-0361630-3049.

## References

[1] SCHOLTZ, R. A. Multiple access with time-hopping impulse modulation. In *Proc. IEEE Military Commun. Conf.*, October, 1993, p. 11-14.

- [2] FCC, Revision of part 15 of the commission's rules regarding ultra-wideband transmission systems. *Federal Communications Commission*, ET Docket, 2002, pp. 98-153.
- [3] KIM, Y., JANG, B., SHIN, C., WOMACK, B. F. Orthonormal pulses for high data rate communications in indoor UWB systems. *IEEE Communications Letter*, 2005, vol. 9, no. 5, p. 405-407.
- [4] DA SILVA, J. A. N., DE CAMPOS, M. L. R. Method for obtaining spectrally efficient orthogonal UWB pulse shapes. In *International Telecommunications Symposium*. Fortaleza-CE (Brazil), September 3-6, 2006.
- [5] GHAVAMI, M., MICHAEL, L. B., KOHNO, R. *Ultra Wideband Signals and Systems in Communication Engineering*. John Wiley & Sons, Ltd, 2004.
- [6] ZHANG, H., LI, W., GULLIVER, T. A. Pulse Position Amplitude Modulation for time-hopping multiple-access UWB communications. *IEEE Trans. on Comm.*, 2005, vol. 53, no. 8.
- [7] ZHANG, H., GULLIVER, T. A. Biorthogonal Pulse Position Modulation for time-hopping multiple-access UWB communications. *IEEE Trans. on Wireless Comm.*, 2005, vol. 4, no. 3.
- [8] MAJHI, S., MADHUKUMAR, A. S. Combining OOK with PSM modulation for TH-UWB radio systems: A performance analysis. *EURASIP Journal on Wireless Comm. and Networking*, 2008.
- [9] MITCHELL, C. J., ABREU, G., KOHNO, R. Combined pulse shape and pulse position modulation for high data rate transmissions in ultra-wideband communications. *International Journal of Wireless Information Networks*, October 2003, vol. 10, no. 4.
- [10] ELTAHER, A., KAISER, TH. Hybrid shape, amplitude, and position modulation for UWB communication systems. *WSEAS Journal on Communications*, July 2004.
- [11] GHAVAMI, M., MICHAEL, L. B., HARUYAMA, S., KOHNO, R. A novel UWB pulse shape modulation system. *Wireless Personal Communications*, 2002, vol. 23, p. 105-120.
- [12] PROAKIS, J. G. *Digital Communications*. 4<sup>th</sup> ed., New York: McGraw-Hill, 2001.
- [13] DILINAR, S., DIVSALAR, D., HAMKINS, J., POLLARA, F. Capacity of Pulse-Position Modulation (PPM) on Gaussian and Webb channels. *TMO Progress Report*, vol. 42-142, August 15, 2000.
- [14] DURISI, G., ROMANO, G. On the validity of Gaussian approximation to characterize the multiuser capacity of UWB TH PPM. In *Proc. IEEE Conf. Ultra Wideband Systems and Technology*, 2002, pp. 157-161.
- [15] LI ZHAO, HAIMOVICH, A. M. Capacity of  $M$ -ary PPM ultra-wideband communications over AWGN channels. In *Proc. IEEE 54<sup>th</sup> Vehicular Technology Conference*. Atlantic City (USA), October 2001, vol. 2, p. 1191-1195.
- [16] PROAKIS, J. G., SALEHI, M. *Contemporary Communication Systems Using MATLAB*. PWS publishing company, 1998.
- [17] ABEDI, O., NIELSEN, J. UWB data rate and channel capacity in modulation schemes. In *Canadian Conference on Electrical and Computer Engineering*. May 2006, p. 1809 – 1816.

## About Authors...

**Marijan HERCEG** was born in Osijek, Croatia, in 1978. He received the B.S. degree in Electrical Engineering from the Faculty of Electrical Engineering in Osijek, Croatia in 2002. He is currently working towards Ph.D. degree in Communication and Informatics at the Faculty of Electrical

Engineering in Osijek, Croatia. His research interests are advanced modulation techniques like power efficient modulations for ultra-wide band (UWB) and FPGA programming for communications applications.

**Tomislav MATIĆ** was born in Osijek, Croatia, in 1978. He received his B.S. degree from the Faculty of Electrical Engineering in Osijek in 2002. Currently he is assistant at the Department of Communications, Faculty of Electrical Engineering in Osijek, where he is working towards PhD degree in Communications. His current research interests are A/D conversion, sigma-delta A/D converters and FPGA programming for communication applications.

**Tomislav ŠVEDEK** received BSc, MSc and PhD degrees from the Faculty of Electrical Engineering Zagreb, University of Zagreb, Croatia. He joined the Institute for Electronics, Telecommunications and Automation (IETA) RIZ Zagreb, in 1975 as development engineer, PTT Project buerou, Zagreb in 1980 as project leader, the Electrotechnical Institute of Rade Končar, Department for Design of Integrated Circuits in 1986 as ASIC supervisor, and the Faculty of Electrical Engineering, University of Osijek in 1993, as Full professor for Electronic Circuits and Microelectronics. His scientific interests are design and testability of ASICs, microelectronic RF circuits, and digital modulation methods.